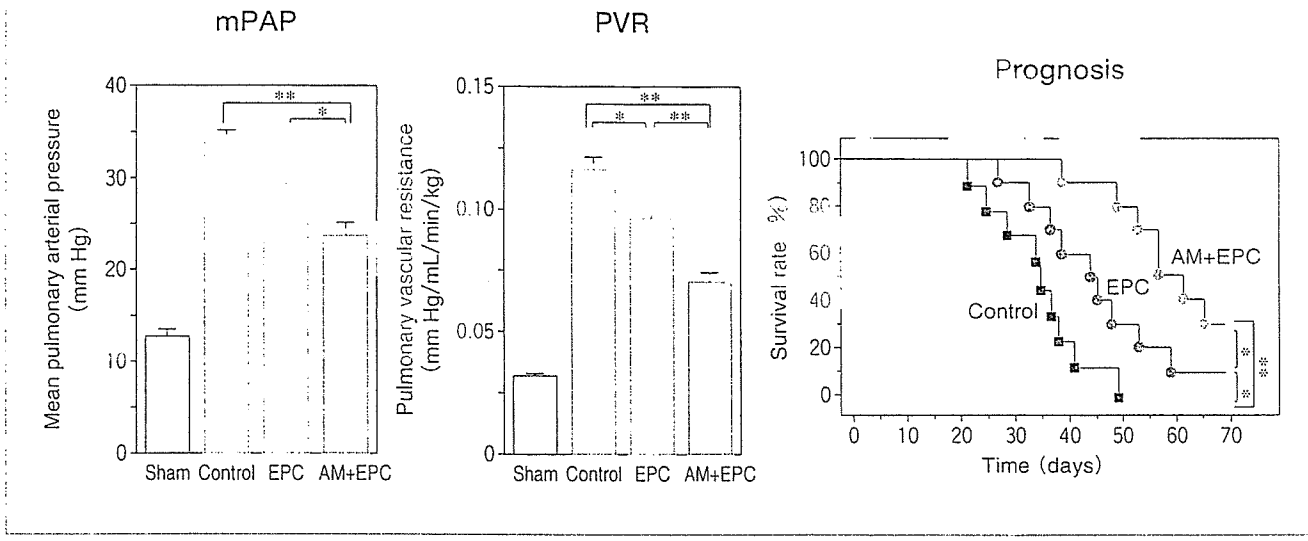

図7　アドレノメデュリン(AM)遺伝子導入 EPC の移植による平均肺動脈圧(mPAP)，肺血管抵抗(PVR)，肺高血圧ラットの予後改善効果

Sham：正常ラット、Control：モノクロタリン肺高血圧ラットへ vehicle 投与、
EPC：肺高血圧ラットへ EPC 投与、AM＋EPC：肺高血圧ラットへ AM 遺伝子導入 EPC 投与
P＜0.05、　P＜0.001　　文献 18 より改変、引用

して肺組織選択的に遺伝子導入を可能にし，新たな肺高血圧治療法として期待される．

References

1) Archer S, Rich S : Primary pulmonary hypertension : a vascular biology and translational research "Work in progress". Circulation 102 : 2781-2791, 2000
2) Giaid A, Yanagisawa M, Langleben D, et al : Expression of endothelin-1 in the lungs of patients with pulmonary hypertension. N Engl J Med 328 : 1732-1739, 1993
3) Tuder RM, Cool CD, Geraci MW, et al : Prostacyclin synthase expression is decreased in lungs from patients with severe pulmonary hypertension. Am J Respir Crit Care Med 159 : 1925-1932, 1999
4) Christman BW, McPherson CD, Newman JH, et al : An imbalance between the excretion of thromboxane and prostacyclin metabolites in pulmonary hypertension. N Engl J Med 327 : 70-75, 1992
5) Champion HC, Bivalacqua TJ, D'Souza FM, et al : Gene transfer of endothelial nitric oxide synthase to the lung of the mouse in vivo. Effect on agonist-induced and flow-mediated vascular responses. Circ Res 84 : 1422-1432, 1999
6) Isner JM, Pieczek A, Schainfeld R, et al : Clinical evidence of angiogenesis after arterial gene transfer of phVEGF 165 in patient with ischaemic limb. Lancet 348 : 370-374, 1996
7) Lederman RJ, Mendelsohn FO, Anderson RD, et al : Therapeutic angiogenesis with recombinant fibroblast growth factor-2 for intermittent claudication (the TRAFFIC study) : a randomised trial. Lancet 359 : 2053-2058, 2002
8) Aoki M, Morishita R, Taniyama Y, et al : Therapeutic angiogenesis induced by hepatocyte growth factor : potential gene therapy for ischemic diseases. J Atheroscler Thromb 7 : 71-76, 2000
9) Gerber HP, McMurtrey A, Kowalski J, et al : Vascular endothelial growth factor regulates endothelial cell survival through the phosphatidylinositol 3'-kinase/Akt signal transduction pathway. Requirement for Flk-1/KDR activation. J Biol Chem 273 : 30336-30343, 1998
10) Tuder RM, Chacon M, Alger L, et al : Expression of angiogenesis-related molecules in plexiform lesions in severe pulmonary hypertension : evidence for a process of disordered

angiogenesis. J Pathol 195 : 367-374, 2001
11) Partovian C, Adnot S, Raffestin B, et al : Adenovirus-mediated lung vascular endothelial growth factor overexpression protects against hypoxic pulmonary hypertension in rats. Am J Respir Cell Mol Biol 23 : 762-771, 2000
12) Zhao YD, Campbell AI, Robb M, et al : Protective role of angiopoietin-1 in experimental pulmonary hypertension. Circ Res 92 : 984-991, 2003
13) Ono M, Sawa Y, Matsumoto K, et al : In vivo gene transfection with hepatocyte growth factor via the pulmonary artery induces angiogenesis in the rat lung.Circulation 106 : 1264-1269, 2002
14) Asahara T, Murohara T, Sullivan A, et al : Isolation of putative progenitor endothelial cells for angiogenesis. Science 275 : 964-967, 1997
15) Kawamoto A, Gwon HC, Iwaguro H, et al : Therapeutic potential of ex vivo expanded endothelial progenitor cells for myocardial ischemia. Circulation 103 : 634-637, 2001
16) Stamm C, Westphal B, Kleine HD, et al : Autologous bone-marrow stem-cell transplantation for myocardial regeneration. Lancet 361 : 45-46, 2003
17) Tateishi-Yuyama E, Matsubara H, Murohara T, et al : Therapeutic Angiogenesis using Cell Transplantation (TACT) Study Investigators. Therapeutic angiogenesis for patients with limb ischaemia by autologous transplantation of bone-marrow cells : a pilot study and a randomised controlled trial. Lancet 360 : 427-435, 2002
18) Nagaya N, Kangawa K, Kanda M, et al : Hybrid cell-gene therapy for pulmonary hypertension based on phagocytosing action of endothelial progenitor cells. Circulation 108 : 889-895, 2003
19) Zhao YD, Deng Y, Zhang Q, et al : Regeneration of lung microvasculature by endothelial progenitor cells in experimental pulmonary arterial hypertension (PAH). Circulation Supplement Ⅳ-295, 2003 (abstract)
20) Kitamura K, Kangawa K, Kawamoto M, et al : Adrenomedullin : a novel hypotensive peptide isolated from human pheochromocytoma. Biochem Biophys Res Commun 192 : 553-560, 1993
21) Owji AA, Smith DM, Coppock HA, et al : An abundant and specific binding site for the novel vasodilator adrenomedullin in the rat. Endocrinology 136 : 2127-2134, 1995
22) Ishizaka Y, Ishizaka Y, Tanaka M, et al : Adrenomedullin stimulates cyclic AMP formation in rat vascular smooth muscle cells. Biochem Biophys Res Commun 200 : 642-646, 1994
23) Nakamura M, Yoshida H, Makita S, et al : Potent and long-lasting vasodilatory effects of adrenomedullin in humans : comparisons between normal subjects and patients with chronic heart failure. Circulation 95 : 1214-1221, 1997
24) Nagaya N, Nishikimi T, Uematsu M, et al : Haemodynamic and hormonal effects of adrenomedullin in patients with pulmonary hypertension. Heart 84 : 653-658, 2000
25) Nagaya N, Kyotani S, Uematsu M, et al : Effects of adrenomedullin inhalation on hemodynamics and exercise capacity in patients with primary pulmonary hypertension. Circulation (in press)
26) Tabata Y, Nagano A, Ikada Y. Biodegradation of hydrogel carrier incorporating fibroblast growth factor. Tissue Engin 5 : 127-138, 1999

Available online at www.sciencedirect.com
ScienceDirect
Journal of Molecular and Cellular Cardiology 42 (2007) 88–97
Journal of Molecular and Cellular Cardiology
www.elsevier.com/locate/yjmcc

Original article

Transplantation of mesenchymal stem cells attenuates myocardial injury and dysfunction in a rat model of acute myocarditis

Shunsuke Ohnishi [a,*,1], Bobby Yanagawa [a,1], Koichi Tanaka [a], Yoshinori Miyahara [a], Hiroaki Obata [a,b], Masaharu Kataoka [a], Makoto Kodama [b], Hatsue Ishibashi-Ueda [c], Kenji Kangawa [d], Soichiro Kitamura [e], Noritoshi Nagaya [a,*]

[a] *Department of Regenerative Medicine and Tissue Engineering, National Cardiovascular Center Research Institute, Fujishirodai 5-7-1, Osaka 565-8565, Japan*
[b] *Division of Cardiology, Niigata University Graduate School of Medical and Dental Sciences, Niigata, Japan*
[c] *Department of Pathology, National Cardiovascular Center, Osaka, Japan*
[d] *Department of Biochemistry, National Cardiovascular Center Research Institute, Osaka, Japan*
[e] *Department of Cardiovascular Surgery, National Cardiovascular Center, Osaka, Japan*

Received 11 May 2006; received in revised form 29 August 2006; accepted 2 October 2006
Available online 13 November 2006

Abstract

Acute myocarditis is a non-ischemic inflammatory disease of the myocardium for which there is currently no specific treatment. We have previously shown that mesenchymal stem cells (MSC) can ameliorate heart injury during acute ischemia and in dilated cardiomyopathy; however, the therapeutic potential in acute myocarditis is unclear. In this study, we investigated the ability of MSC to attenuate myocardial injury and dysfunction during the acute phase of experimental myocarditis. Ten-week-old male Lewis rats were injected with porcine myosin to induce myocarditis. Cultured MSC (3×10^6 cells/rat) were injected intravenously 7 days after myosin injection. At 3 weeks, myosin injection resulted in severe inflammation and significant deterioration of cardiac function. MSC transplantation attenuated increases in CD68-positive inflammatory cells and monocyte chemoattractant protein-1 (MCP-1) expression in myocardium, and improved cardiac function in this model. Furthermore, myocardial capillary density was higher in myocarditis tissue, and was further increased by MSC transplantation. *In vitro*, cultured adult rat cardiomyocytes were injured in response to MCP-1, whereas this effect was attenuated by MSC-derived conditioned medium, suggesting cardioprotective effects of MSC acting in a paracrine manner. MSC transplantation attenuated myocardial injury and dysfunction in a rat model of acute myocarditis, at least in part through paracrine effects of MSC.

Keywords: Acute myocarditis; Mesenchymal stem cell; Paracrine effect; Cytokine; Cell death

1. Introduction

Acute myocarditis is a non-ischemic heart disease characterized by myocardial inflammation and edema. This disease is associated with rapidly progressive heart failure, arrhythmias and sudden death [1,2]. Although the early evidence for efficacy of immunoglobulin and interferon therapy appears promising, these results have yet to be demonstrated in randomized or controlled clinical trials. The current options are restricted to supportive care for heart failure or arrhythmias. The lack of specific treatment and the potential severity of the illness emphasize the importance of novel and effective therapeutic strategies for myocarditis.

Mesenchymal stem cells (MSC) are multipotent stem cells present in adult tissues, and have the ability to differentiate into a variety of lineages, including vascular smooth muscle cells, endothelial cells and cardiomyocytes [3,4]. We have previously reported that bone marrow-derived MSC engrafted in experimental myocardial infarction expressed both cardiac and endothelial phenotypes in the heart, and further increased capillary density and decreased the infarct size [5]. Moreover, we have recently demonstrated that monolayered MSC derived from adipose tissue reversed wall thinning in the scar area and improved cardiac function in rats with myocardial infarction [6]. The cardioprotective effects of MSC are known to be mediated

* Corresponding authors. Tel.: +81 6 6833 5012; fax: +81 6 6833 9865.
E-mail addresses: sonsihi@ri.ncvc.go.jp (S. Ohnishi), nnagaya@ri.ncvc.go.jp (N. Nagaya).
[1] Drs Ohnishi and Yanagawa contributed equally to this study.

0022-2828/$ - see front matter © 2006 Elsevier Inc. All rights reserved.
doi:10.1016/j.yjmcc.2006.10.003

not only by their differentiation into vascular cells and cardiomyocytes, but also by their ability to supply large amounts of angiogenic, anti-apoptotic and mitogenic factors [5–7]. These findings suggest the therapeutic potential of MSC for heart failure. However, whether intravenously transplanted MSC attenuate myocardial inflammation and cardiac dysfunction in acute myocarditis remains unknown.

In the present study, we used porcine myosin-induced acute myocarditis in Lewis rats. This model closely resembles human giant cell myocarditis, a frequently fatal disorder characterized by multinucleated giant cells in the myocardium [8]. To examine the therapeutic potential of MSC in the acute phase of myocarditis, MSC were intravenously injected into rats 7 days after myosin injection.

Thus, the purposes of this study were 1) to investigate whether intravenous transplantation of MSC improves cardiac function and pathological findings including myocardial inflammation in rats with myosin-induced myocarditis, and 2) to investigate the underlying mechanisms responsible for the effects of MSC.

2. Materials and methods

2.1. Animals

Ten-week-old male Lewis rats (Japan SLC, Hamamatsu, Japan) were used in all experiments, and were maintained in our animal facilities. The experimental protocols were approved by The Animal Care Committee of the National Cardiovascular Center.

2.2. Preparation of cardiac myosin

Purified cardiac myosin from the ventricular muscle of pig hearts was prepared according to a procedure described previously [8]. The antigen was dissolved at a concentration of 20 mg/ml in phosphate-buffered saline (PBS) containing 0.3 M KCl, mixed with an equal volume of complete Freund's adjuvant containing 11 mg/ml *Mycobacterium tuberculosis* (Difco Laboratories, Sparks, MD, USA). Rats were anesthetized with an intraperitoneal injection of 20 mg/kg sodium pentobarbital, and 0.1 ml of the antigen-adjuvant emulsion was injected into the each footpad.

2.3. Acute myocarditis model

Forty-five rats were randomly divided into three groups and received the following treatment: 1) 0.2 ml saline and sham surgery (Sham group, $n=15$), 2) 0.2 ml cardiac myosin antigen and sham surgery (MyoC group, $n=15$), and 3) 0.2 ml cardiac myosin followed by MSC transplantation 7 days post-myosin injection (MyoC+MSC group, $n=15$). Rats were weighed and observed daily for signs of morbidity and for death.

2.4. Preparation and transplantation of bone marrow-derived MSC

MSC were prepared as described previously [5]. Briefly, bone marrow cells were isolated by flushing out the femoral and tibial cavities with PBS, and plated onto 10-cm dishes in complete culture medium: Dulbecco's Modified Eagle's Medium (DMEM), 15% fetal bovine serum, 100 U/ml penicillin and 100 μg/ml streptomycin. Five days after plating, non-adherent cells were removed, and adherent cells were further propagated for 4 to 5 passages.

Seven days after myosin injection, MSC (3×10^6 cells) or vehicle (0.9% saline) was intravenously administered via the jugular vein. Sham rats also received saline administration but without myosin injection.

2.5. Hemodynamic studies

Hemodynamic studies were performed on day 21 post-myosin injection. Anesthesia was maintained with an intraperitoneal injection of 20 mg/kg sodium pentobarbital, and a 1.5 Fr micromanometer-tipped catheter was placed in the left ventricle through the right carotid artery (Millar Instruments, Houston, TX, USA). Heart rate (HR) was also monitored by electrocardiography. HR, mean arterial pressure (MAP), left ventricular systolic pressure (LVSP), left ventricular end-diastolic pressure (LVEDP), maximum dP/dt (Max dP/dt) and minimum dP/dt (Min dP/dt) were used as indices of hemodynamics, and recorded simultaneously during ventilation after a minimum equilibration period of 20 min.

2.6. Echocardiographic studies

Echocardiography was performed on day 21 post-myosin injection. Rats were anesthetized with an intraperitoneal injection of 20 mg/kg sodium pentobarbital. A 12 MHz probe was placed at the left 4th intercostal space for M-mode imaging using 2D echocardiography (Sonos 5500, Philips, Bothell, WA, USA). Left ventricular systolic dimension (LVDs), left ventricular diastolic dimension (LVDd), anterior wall thickness (AWT), posterior wall thickness (PWT) and ejection fraction (EF) were measured, and taken as an average of three beats. Fractional shortening (%FS) was calculated as $(LVDd-LVDs)/LVDd\times100$.

2.7. Histological examination

The heart was excised above the origin of the great vessels, and heart weight and body weight were recorded on day 21 post-myosin injection. Portions of the midventricular heart, spleen, pancreas, kidney and liver were fixed with 4% paraformaldehyde, embedded in paraffin, sectioned at 4-μm thickness, stained with either hematoxylin and eosin (H & E) or Masson's trichrome, and subjected to immunohistochemical staining. H & E-stained sections were evaluated by a cardiovascular pathologist (H.I.-U.) for the characterization of myocardial injury and inflammation without knowledge of the experimental groups, on the following scale: 0, absent or questionable presence; 1, limited focal distribution; 2–3, intermediate severity; and 4, coalescent and extensive foci throughout the entire transversely sectioned ventricular tissue.

2.8. Immunohistochemical study

Paraffin-embedded heart sections were washed in increasing concentrations of ethanol and then with PBS. Sections were incubated with Protein Block (DakoCytomation, Glostrup, Denmark), then with mouse anti-rat von Willebrand Factor (vWF) (DakoCytomation), CD68 (DakoCytomation) or monocyte chemoattractant protein-1 (MCP-1) (BD Biosciences Pharmingen, San Jose, CA, USA) antibody in diluent for 40 min, followed by incubation with horseradish peroxidase (HRP)-linked rabbit anti-mouse IgG (DakoCytomation) for 30 min. Sections were visualized using 0.5% diaminobenzidine and 0.03% hydrogen peroxide, and counterstained with hematoxylin. The numbers of CD68-stained cells and vWF-stained capillaries were determined in 10 randomly selected fields (×200).

2.9. Enzyme-linked immunosorbent assay (ELISA)

Serum MCP-1 level of rats on day 21 post-myosin injection was measured using a Rat MCP-1 ELISA kit (Biosource International, Carmarillo, CA, USA). Vascular endothelial growth factor (VEGF) and hepatocyte growth factor (HGF) levels in the supernatant of MSC culture (2.3×10^5 cells in 10-cm dish cultured for 48 h) were measured using ELISA kits, according to the manufacturers' protocols (HGF, Institute of Immunology, Tokyo, Japan; VEGF, R&D Systems, Minneapolis, MN, USA).

2.10. Isolation of cardiomyocytes

Ventricular cardiomyocytes were obtained as described previously with modification [9]. Briefly, after heparinization by intraperitoneal injection of 1000 U/kg heparin sodium, the heart was rapidly excised, and pulmonary, connective and other noncardiac tissues were removed. The heart was then mounted on the cannula of a modified Langendorff apparatus and perfused with buffer containing 0.75 mg/ml collagenase type I (Worthington, Lakewood, NJ, USA), 0.5 mg/ml hyaluronidase (Sigma) and 1% bovine serum albumin (fraction V, ICN, Aurora, OH, USA), in a recirculating fashion for 3 h. After the perfusion sequence, the heart was removed from the perfusion apparatus, the atrium was removed, and gently minced. The enzyme-containing buffer was harvested and the cardiomyocytes resuspended in fresh buffer. The calcium concentration in the suspension was raised stepwise to 1.2 mM. Quiescent, calcium-tolerant cardiomyocytes were gravitationally separated from any nonventricular cells and resuspended in complete culture medium. The culture medium was exchanged for fresh medium to remove the damaged myocytes that failed to attach 3 h after plating. After this procedure, 80% to 90% myocytes were viable and showed rod-shape.

2.11. Cardiomyocyte stimulation and MTS assay

To assess cardioprotective effects of MSC acting in a paracrine manner, we investigated whether conditioned medium obtained from MSC culture attenuated MCP-1-induced cardiomyocyte injury. Cardiomyocytes were plated on 96-well plates (1×10^3 viable cells/well) precoated with laminin (BD Biosciences Pharmingen). After 3 h, the medium was changed to fresh DMEM containing 15% FBS or conditioned medium obtained from MSC culture, with or without 50 ng/ml MCP-1 (R&D Systems, Minneapolis, MN, USA). After 24 h, the cellular level of 3-(4,5-dimethylthiazol-2-yl)-5-(3-carboxymethoxyphenyl)-2-(4-sulfophenyl)-2H-tetrazolium (MTS), indicative of the mitochondrial function in living cells and cell viability, was measured ($n=6$) with a CellTiter96 AQueous One Kit (Promega, Madison, WI, USA) and a Microplate Reader (490 nm, Bio-Rad, Hercules, CA, USA).

2.12. In vitro apoptosis assay

Terminal dUTP nick end labeling (TUNEL) assay (ApopTag Fluorescein In Situ Apoptosis Detection Kit, Chemicon International, Temecula, CA, USA) was performed to evaluate apoptosis of cultured cardiomyocytes. After incubation for 24 h, cardiomyocytes were fixed in 1% paraformaldehyde, and TUNEL staining was performed for detection of apoptotic nuclei according to the manufacturer's

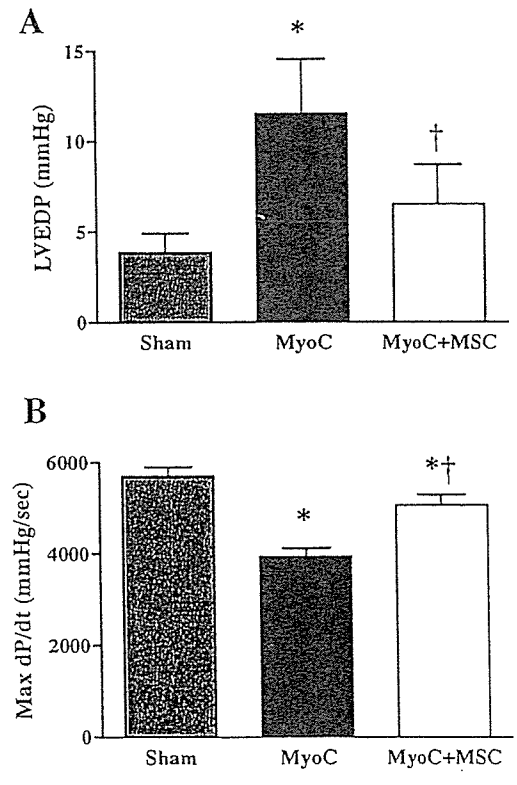

Fig. 1. Effects of MSC transplantation on hemodynamic parameters in acute myocarditis. (A) Left ventricular end-diastolic pressure (LVEDP) and (B) maximum dP/dt (Max dP/dt) were measured in sham-operated rats given vehicle (Sham group), myosin-treated rats given vehicle (MyoC group), and myosin-treated rats given MSC (MyoC+MSC group). Values are mean±S.E. $^*P<0.05$ *vs* Sham, $^\dagger P<0.05$ *vs* MyoC group.

Table 1
Physiological parameters in three experimental groups

	Sham	MyoC	MyoC+MSC
HW/BW (g/kg)	2.9±0.3	6.4±0.3*	4.7±0.3*,†
HR (bpm)	446±11	363±14*	442±12*,†
MAP (mm Hg)	108±3	87±3*	108±4†
LVSP (mm Hg)	130±2	105±4*	125±4†
Min d*P*/d*t* (mm Hg/s)	−5440±199	−3097±183*	−4617±171*,†

Sham, sham-operated rats given vehicle; MyoC, myosin-treated rats given vehicle; MyoC+MSC, myosin-treated rats given MSC (3×10^6 cells); HW/BW, heart weight to body weight ratio; HR, heart rate; MAP, mean arterial pressure; LVSP, left ventricular systolic pressure; Mim d*P*/d*t*, minimum d*P*/d*t*. Data are mean±S.E. *$P<0.05$ *vs* Sham, †$P<0.05$ *vs* MyoC group.

instructions. The cells were then mounted in medium containing DAPI. Randomly selected microscopic fields ($n=5$) were evaluated to calculate the ratio of TUNEL-positive cells to total cells.

Table 2
Echocardiographic findings in three experimental groups

	Sham	MyoC	MyoC+MSC
LVDs (mm)	3.1±0.1	5.0±0.4*	3.8±0.2†
EF (%)	74.9±1.2	56.6±3.4*	71.2±3.5†
AWT diastole (mm)	1.9±0.1	3.0±0.2*	3.0±0.3*
PWT diastole (mm)	1.9±0.1	3.4±0.1*	2.7±0.2*,†

Sham, sham-operated rats given vehicle; MyoC, myosin-treated rats given vehicle; MyoC+MSC, myosin-treated rats given MSC (3×10^6 cells); LVDs, left ventricular systolic dimension; EF, ejection fraction; AWT, anterior wall thickness; PWT, posterior wall thickness. Data are mean±S.E. *$P<0.05$ *vs* Sham, †$P<0.05$ *vs* MyoC group.

2.13. Creatine kinase (CK) activity assay

CK activity in culture media was measured after incubation of cardiomyocytes for 24 h ($n=5$), using the enzyme measurement kit (Kanto Chemical, Tokyo, Japan).

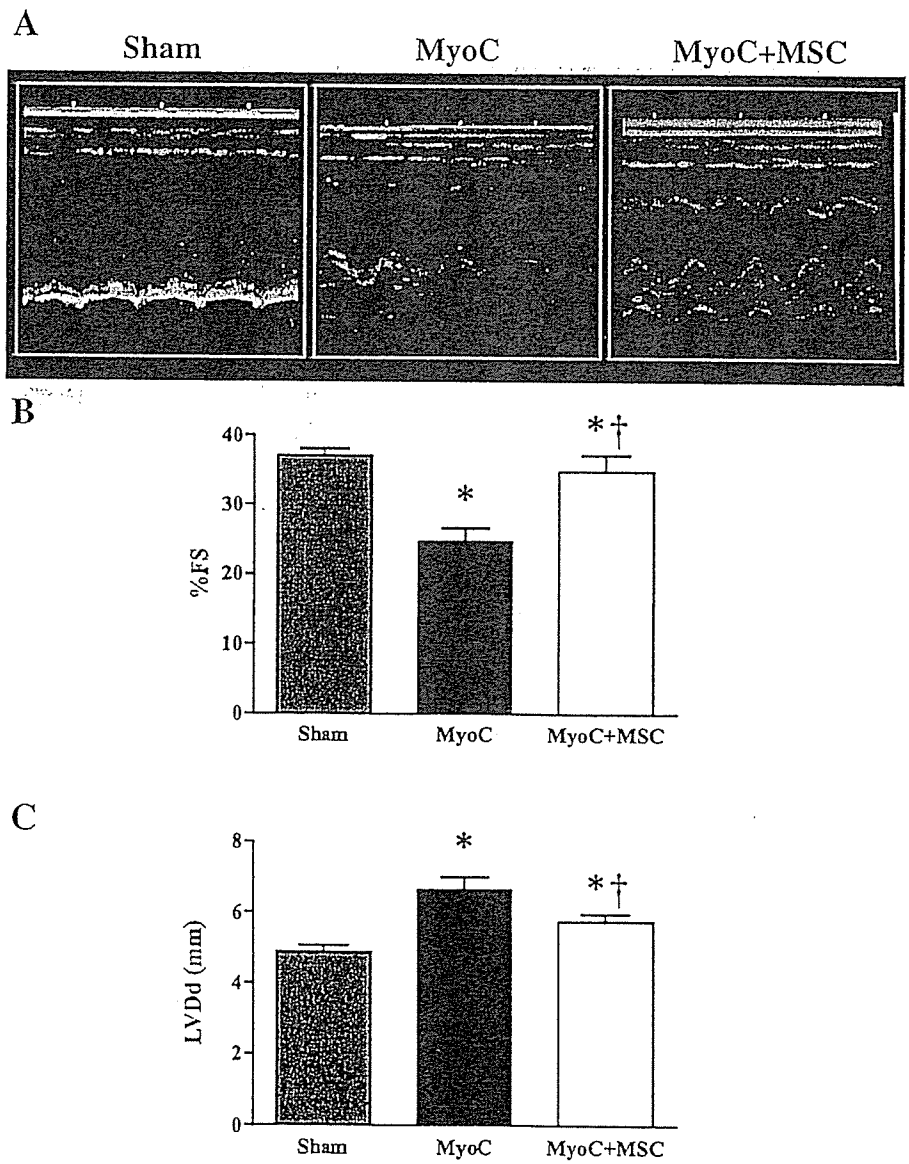

Fig. 2. Effects of MSC transplantation on echocardiographic parameters in acute myocarditis. (A) Representative echocardiographic images showing wall thickening and poor movement in the MyoC group, and improvement of cardiac contractility in the MyoC+MSC group. (B and C) MSC transplantation significantly improved fractional shortening (%FS) and left ventricular diastolic dimension (LVDd). Values are mean±S.E. *$P<0.05$ *vs* Sham, †$P<0.05$ *vs* MyoC group.

2.14. Statistical analysis

Data were expressed as mean ± standard error (S.E.). Comparisons of parameters among groups were made by one-way ANOVA, followed by Newman–Keuls' test. Differences were considered significant at $P<0.05$.

3. Results

3.1. Improvement in cardiac function by MSC transplantation

Two of 15 rats in the MyoC group died on day 19 and day 21 post-myosin injection, respectively, whereas the MyoC+MSC group had no mortality. At 3 weeks post-myosin injection, the MyoC group showed increased heart weight/body weight ratio (HW/BW) and LVEDP, and decreased MAP and Max d*P*/d*t* compared with the Sham group, indicating the presence of acute heart failure in this model (Fig. 1 and Table 1). These parameters subsequently returned to baseline with MSC transplantation (MyoC+MSC group). On echocardiography, the MyoC group showed an increase in LVDs and LVDd, and a significant reduction in %FS and EF (Fig. 2 and Table 2). MSC transplantation significantly improved these parameters (MyoC+MSC group).

3.2. Attenuation of myocardial inflammation by MSC transplantation

Myocardial necrosis and tissue granulation as well as giant cell infiltration and edema were markedly increased in our model of acute myocarditis (Fig. 3A). MSC transplantation significantly attenuated these changes observed in the MyoC group. MSC-transplanted hearts exhibited a consistent tendency for a reduction of tissue granulation, inflammation and edema, on blinded histological grading by a cardiovascular pathologist (H.I-U.), as compared to the MyoC group (Fig. 3B). Hearts showed limited fibrosis in the MyoC group, and this observation was not significantly attenuated by MSC

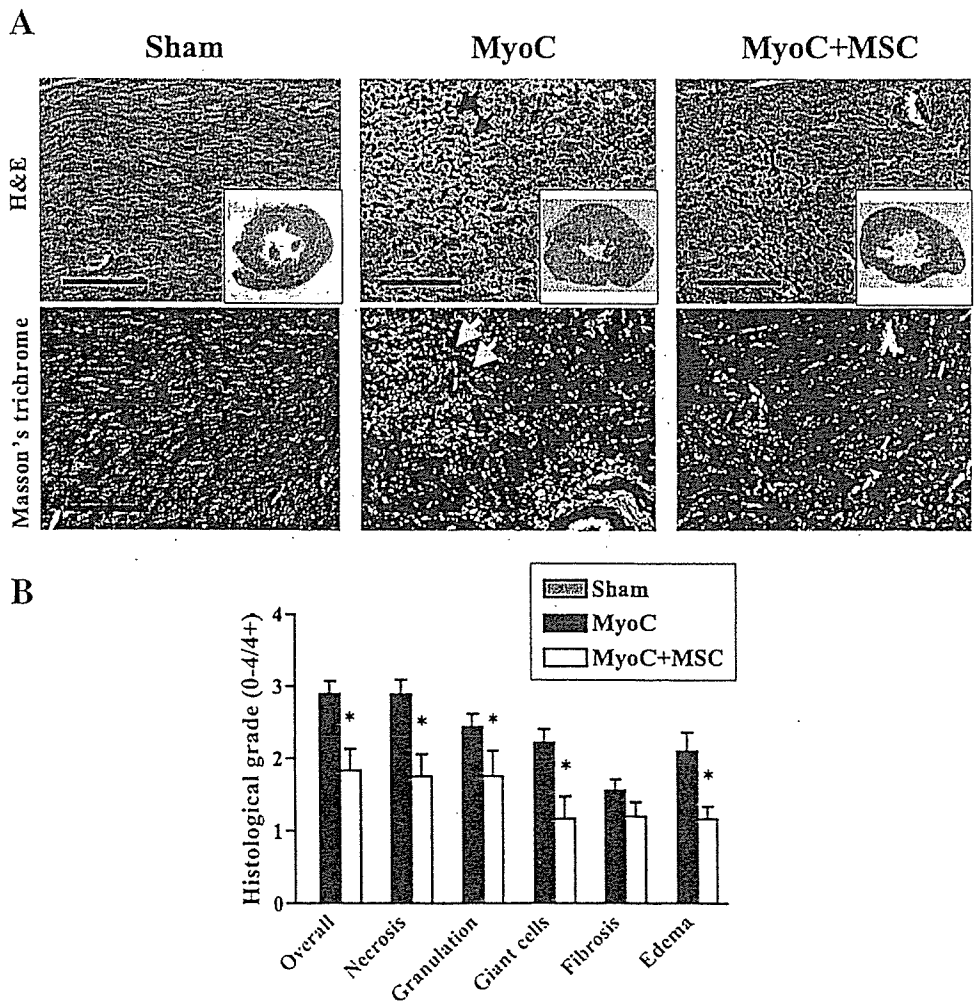

Fig. 3. Effects of MSC transplantation on pathological changes in acute myocarditis. (A) Representative myocardial sections show markedly decreased inflammation and tissue necrosis (H & E) and a comparable degree of early fibrosis (Masson's trichrome) after MSC transplantation (MyoC+MSC) as compared to control (MyoC, arrows). Insets are transverse sections of myocardium. Scale bars: 50 μm. (B) Semi-quantitative histological grades for necrosis and tissue granulation as well as for infiltration of giant cells and edema were significantly lower after MSC transplantation (MyoC+MSC) compared to control (MyoC). Sham tissues exhibited no measurable pathological change. Values are mean±S.E. $^{*}P<0.05$ *vs* Sham, $^{\dagger}P<0.05$ *vs* MyoC group.

transplantation, possibly because of the acute nature of this experiment (Fig. 3B).

Notably, marked histiocytic infiltration was demonstrated by CD68-positive cells, including multinucleated giant cells, in myocarditis (MyoC group), and this was significantly attenuated by MSC transplantation (Figs. 4A and B). In myocarditis, there was an increase in MCP-1 expression localized to the vascular endothelium and also in cardiomyocytes surrounding areas of inflammation (Fig. 5A). The hearts in the MyoC+MSC group showed a partial decrease in MCP-1 expression. Serum MCP-1 level was greatly increased in the MyoC group, whereas the increase was significantly attenuated in the MyoC+MSC group (Fig. 5B).

3.3. Effect of MSC on angiogenesis

To investigate the angiogenic effect of MSC transplantation in the myocardium, immunohistochemical analysis of vWF was performed. Capillary density was increased in the MyoC group (Figs. 6A and B). Notably, in MSC-transplanted tissues, capillary density was increased compared to that in the MyoC group. The clustering of relatively small vessels seen in MSC-transplanted hearts was indicative of recent neovascularization.

3.4. Cardioprotective effects of MSC in paracrine manner

Because MSC transplantation had anti-inflammatory and tissue-protective effects and induced angiogenesis, some paracrine effects were expected. To confirm the paracrine effects of MSC *in vitro*, cardiomycytes were isolated from adult rats, and cultured with MCP-1 in the standard medium or in the conditioned medium obtained from MSC culture. The standard medium containing MCP-1 resulted in a decrease in viable cardiomyocytes; however, MSC-derived conditioned medium containing MCP-1 attenuated the decrease in viable cardiomyocytes (Fig. 7A). TUNEL staining showed that the standard medium containing MCP-1 markedly induced apoptosis of cardiomyocytes (Figs. 7B and C). However, the conditioned medium of MSC significantly attenuated MCP-1-induced cardiomyocyte apoptosis. In addition, CK activity in standard medium containing MCP-1 was significantly increased, whereas the conditioned medium markedly attenuated the CK activity induced by MCP-1 (Fig. 7D).

To investigate whether MSC secreted angiogenic and anti-fibrotic factors, VEGF and HGF levels in MSC culture were measured by ELISA assay. MSC secreted large amounts of VEGF and HGF compared to standard medium, respectively (Fig. 7E).

4. Discussion

In this study, we focused on the therapeutic potential of MSC transplantation in the acute phase of myocarditis. We showed that 1) MSC transplantation 1 week after myosin injection improved cardiac function and attenuated pathological findings including myocardial inflammation, and that 2)

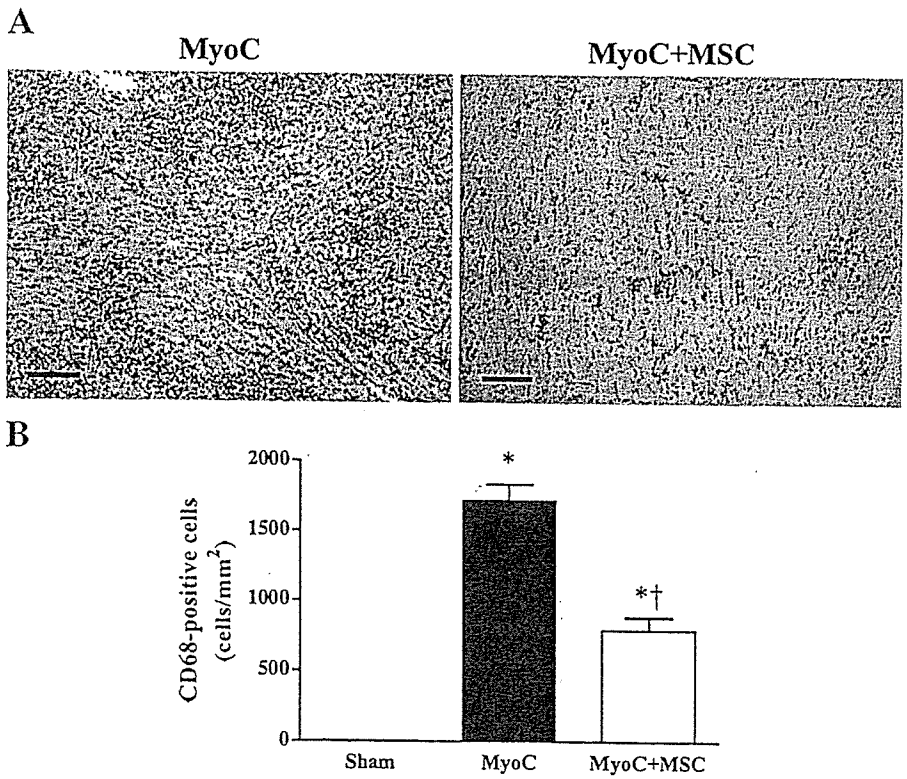

Fig. 4. Effects of MSC transplantation on myocardial CD68 expression in acute myocarditis. (A) Representative myocardial sections immunohistochemically stained for CD68 demonstrate a marked decrease in CD68-positive cells, including giant cells, after MSC transplantation (MyoC+MSC) as compared to control (MyoC). Scale bars: 100 μm. (B) Semi-quantitative counts of CD68-positive cells demonstrate a significant reduction in the MyoC+MSC group. Values are mean±S.E. $^{*}P<0.05$ *vs* Sham, $^{\dagger}P<0.05$ *vs* MyoC group.

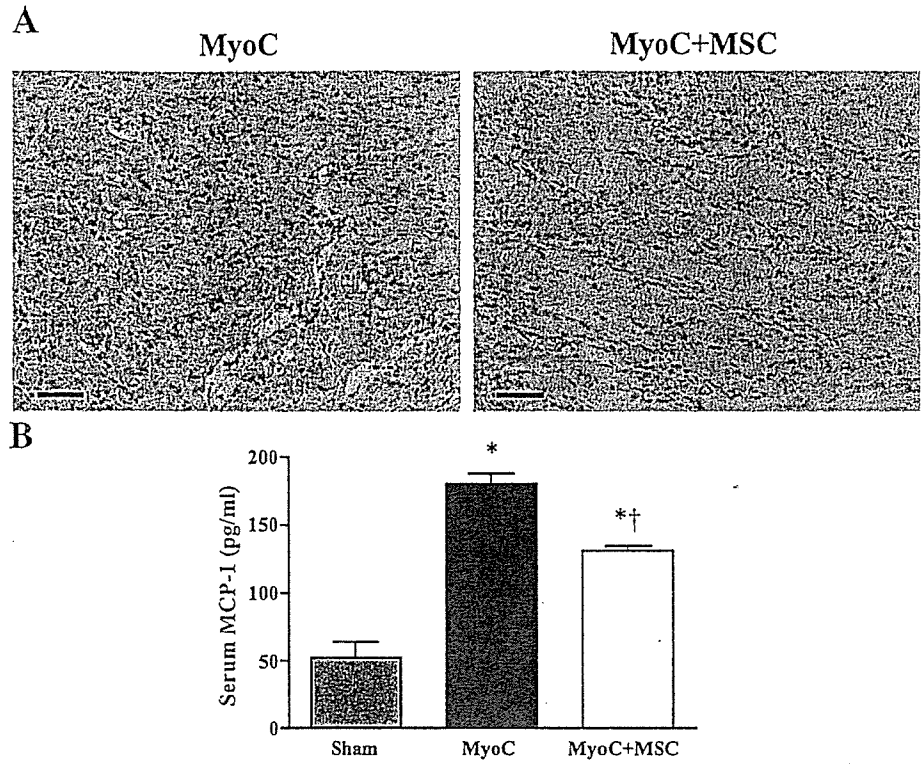

Fig. 5. Effects of MSC transplantation on myocardial MCP-1 expression and serum MCP-1 level. (A) Representative MCP-1-stained myocardial sections from MyoC and MyoC+MSC groups. Scale bars: 50 μm. (B) Serum level of MCP-1 measured by ELISA. Values are mean±S.E. *$P<0.05$ *vs* Sham, †$P<0.05$ *vs* MyoC group.

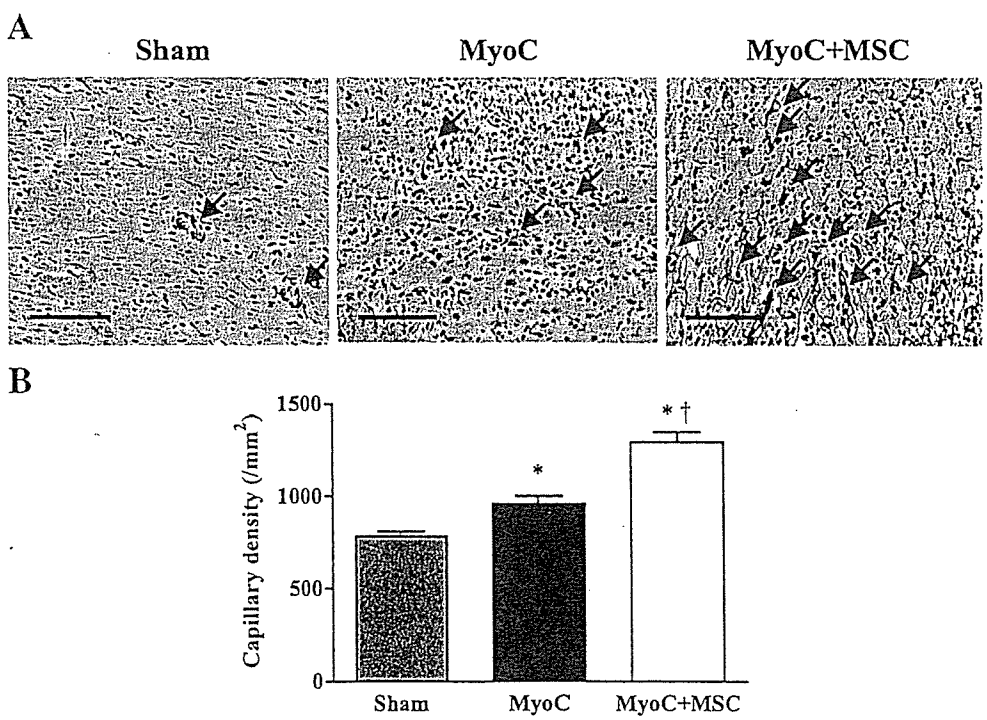

Fig. 6. Effects of MSC on neovascularization. (A) Representative myocardial sections immunohistochemically stained for vWF showing increased microvasculature (arrows) in control hearts (MyoC), which was more marked after MSC transplantation (MyoC+MSC). Scale bars: 50 μm. (B) Capillary density measured in 10 random representative high-power fields showing a significant increase in control (MyoC) and a further increase after MSC transplantation (MyoC+MSC) over the Sham group. Values are mean±S.E. *$P<0.05$ *vs* Sham, †$P<0.05$ *vs* MyoC group.

MSC had cardioprotective effects acting in a paracrine manner.

The rat model of myosin-induced experimental myocarditis provides a model that resembles human giant cell myocarditis [8,10]. Although the majority of acute myocarditis is linked to a viral infection such as coxsackievirus B3, this viral infection can in some cases cause an autoimmune myocarditis with chronic myocardial inflammation without viral persistence, due to the exposure of cardiac autoantigens to the immune system [11,12]. This myocarditis model is triphasic, consisting of an antigen priming phase from days 0–14, an autoimmune response phase from days 14–21, and a reparative phase thereafter, associated chronically with a dilated cardiomyopathy phenotype [13]. In our previous study, MSC were transplanted at the reparative

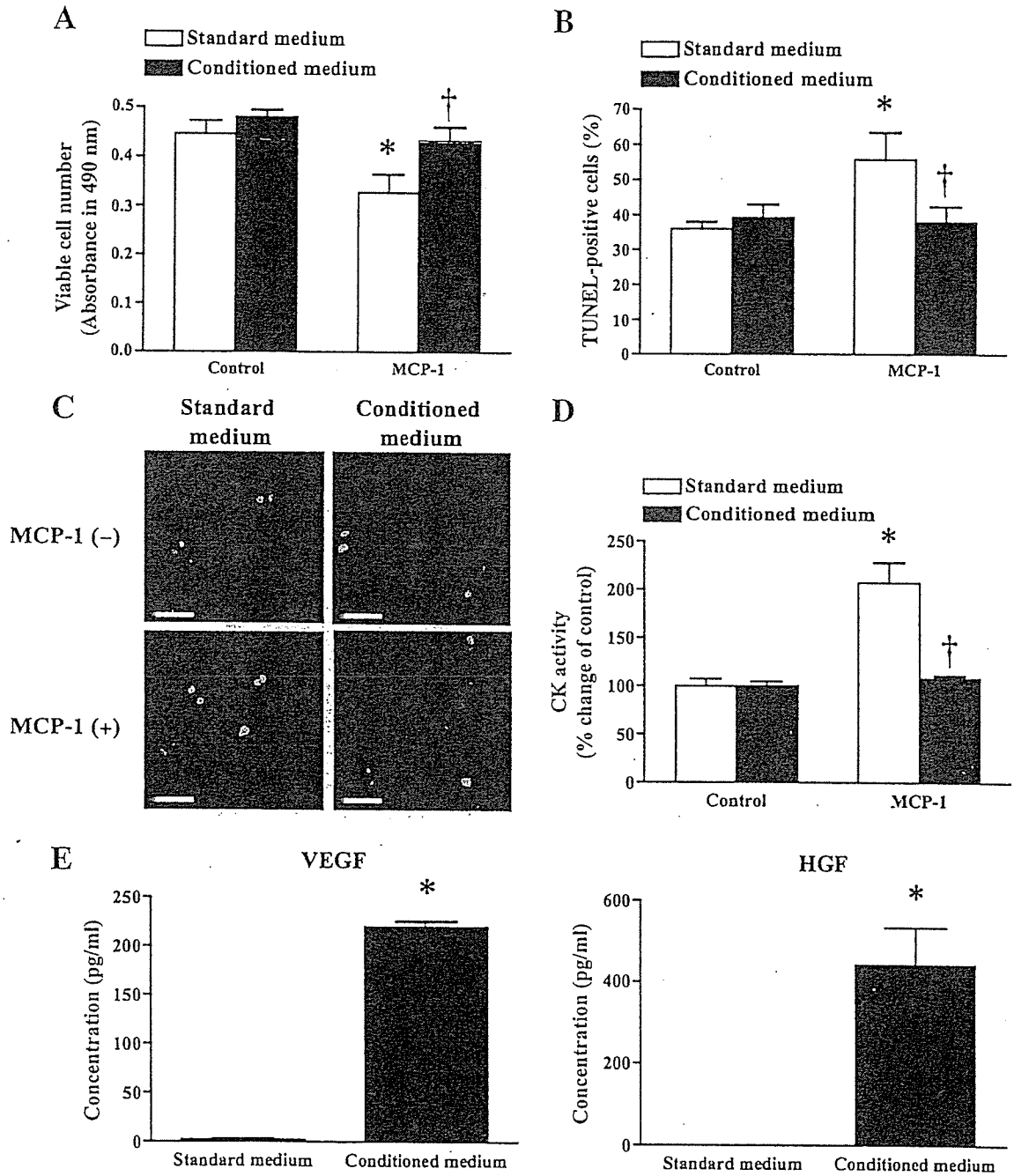

Fig. 7. Effects of MSC on MCP-1-induced cardiomyocyte injury *in vitro*. (A) MTS assay after 24 h of culture with or without MCP-1 in standard medium *vs* MSC conditioned medium. $^{*}P<0.05$ *vs* control in standard medium, $^{\dagger}P<0.05$ *vs* MCP-1 in conditioned medium. (B) Quantitative analysis of TUNEL staining after 24 h of culture with or without MCP-1 in standard medium *vs* MSC conditioned medium. $^{*}P<0.05$ *vs* control in standard medium, $^{\dagger}P<0.05$ *vs* MCP-1 in standard medium. (C) Representative TUNEL staining show increased apoptotic cardiomyocytes (green) cultured with MCP-1 in standard medium, which was attenuated by MSC conditioned medium. Nuclei were counterstained with DAPI (blue). Scale bars: 50 μm. (D) CK activity after 24 h of culture with or without MCP-1 in standard medium *vs* MSC conditioned medium. $^{*}P<0.05$ *vs* control in standard medium, $^{\dagger}P<0.05$ *vs* MCP-1 in standard medium. (E) ELISA for VEGF and HGF secreted from cultured MSC as compared to standard medium. $^{\dagger}P<0.05$ *vs* standard medium.

phase with a dilated cardiomyopathy phenotype, by direct injection into the myocardium [7]. In the present study, however, MSC were transplanted 1 week following myosin injection, corresponding to the acute phase of myocarditis, by intravenous injection, because this model is more relevant to clinical situations. Myosin injection caused acute heart failure as indicated by increased LVEDP and decreased Max d*P*/d*t* and %FS, and 2 out of 15 rats died; however, intravenous injection of MSC in the acute phase significantly improved the heart failure as determined by improvement of these parameters, and no death was observed.

Wang et al. have shown that embryonic stem (ES) cells transplanted into a mouse model of myocarditis regenerate cardiomyocytes, decrease inflammation and increase survival, possibly through migration of ES cells and differentiation into cardiomyocytes [14]. In the present study, we examined the therapeutic potential of transplanted MSC, which are more applicable to clinical situations than ES cells, in a rat model of acute myocarditis. Recent studies have demonstrated that autologous or allogeneic MSC strongly suppress T-lymphocyte proliferation [15,16]. These findings raise the possibility that MSC have the ability to attenuate inflammatory responses. Interestingly, the present study demonstrated that transplantation of MSC attenuated the infiltration of CD68-positive inflammatory cells and the expression of MCP-1 in a rat model of acute myocarditis. MCP-1 is a member of the C–C subfamily of chemokines with chemoattractant activity for major inflammatory cells, and is known to play an important role in the induction of experimental acute myocarditis [17,18]. Cardiac-targeted expression of MCP-1 results in monocyte/macrophage infiltration into the heart, and causes interstitial fibrosis and ventricular chamber dilation [19]. In the myosin-induced acute myocarditis model, MCP-1 expression is increased in the heart from days 15–27 post-myosin injection, and serum MCP-1 level is elevated from days 15–24 [18]. In consistent with this report, our model showed an increase in MCP-1 in the heart and serum on day 21 post-myosin injection, and MSC transplantation attenuated the increase in MCP-1 and the infiltration of CD68-positive inflammatory cells. Furthermore, earlier studies have shown that MSC express CCR2, the receptor for MCP-1, and that MCP-1 promotes the migration of MSC that express CCR2 [20,21]. Thus, it is speculated that MSC secrete some anti-inflammatory factors in response to MCP-1; however, the precise mechanisms for the anti-inflammatory effect still remains to be elucidated.

Because MCP-1 plays an important role in this myosin-induced myocarditis model, we examined the direct effect of MCP-1, besides its chemoattractant activity, on adult rat cardiomyocytes. Our *in vitro* experiment demonstrated that MCP-1 stimulation on cardiomyocytes resulted in an increase of cell injury and death, whereas MSC-derived conditioned medium attenuated these effects. It has been reported that CCR2 expression is increased in the failing myocardium, and MCP-1 stimulation on cardiomyocytes induces other inflammatory cytokines such as IL-1β and IL-6, which may reduce cardiomyocyte contractility partly via induction of apoptosis [22–25]. In addition, our previous and present study demonstrated that cultured MSC secreted large amounts of angiogenic and anti-apoptotic factors such as VEGF, HGF, insulin-like growth factor-1 and adrenomedullin [7]. Furthermore, a recent study demonstrated that conditioned medium obtained from MSC culture had cardioprotective effect [26]. Taken together, although various factors might be involved, MSC might have cardioprotective effects in a paracrine manner in response to MCP-1.

In the present study, MSC transplantation increased capillary density in the myocardium. Improvement in myocardial vascular supply has been shown to decrease necrosis and inflammation in viral myocarditis [8,27,28]. We have previously reported increased capillary density associated with improved cardiac function and decreased infarct size following MSC transplantation in a rat model of myocardial infarction [5]. These results suggest that MSC-induced neovascularization may have contributed to the improvement of cardiac function in this rat model of acute myocarditis. However, when PKH26 dye-labeled MSC were intravenously injected in rats with acute myocarditis, only a small fraction of PKH26-labeled cells were positive for troponin T 2 weeks after transplantation (data not shown). Our previous study demonstrated that ~3% of the intravenously administered MSCs were incorporated into the heart 24 h after transplantation in rats with acute myocardial infarction [5]. Although the animal model and the evaluation time were different, our present study showed that only a small number of administered MSC was differentiated into endothelial cells or cardiomyocytes, thus the contribution of the differentiated MSC to the improvement of cardiac function in this model appears to be rather insignificant.

In conclusion, MSC transplantation attenuated myocardial injury and dysfunction in a rat model of acute myocarditis, at least in part through paracrine effects of MSC.

Acknowledgments

This work was funded by a post-doctoral fellowship from the Japan Society for the Promotion of Science, and research grants for Cardiovascular Disease (16C-6, 17C-1 and 18C-1) and Human Genome Tissue Engineering 009 from the Ministry of Health, Labor and Welfare.

References

[1] Levi D, Alejos J. Diagnosis and treatment of pediatric viral myocarditis. Curr Opin Cardiol 2001;16:77–83.
[2] Feldman AM, McNamara D. Myocarditis. N Engl J Med 2000;343:1388–98.
[3] Pittenger MF, Mackay AM, Beck SC, Jaiswal RK, Douglas R, Mosca JD, et al. Multilineage potential of adult human mesenchymal stem cells. Science 1999;284:143–7.
[4] Le Blanc K, Pittenger M. Mesenchymal stem cells: progress toward promise. Cytotherapy 2005;7:36–45.
[5] Nagaya N, Fujii T, Iwase T, Ohgushi H, Itoh T, Uematsu M, et al. Intravenous administration of mesenchymal stem cells improves cardiac function in rats with acute myocardial infarction through angiogenesis and myogenesis. Am J Physiol: Heart Circ Physiol 2004;287:H2670–6.

[6] Miyahara Y, Nagaya N, Kataoka M, Yanagawa B, Tanaka K, Hao H, et al. Monolayered mesenchymal stem cells repair scarred myocardium after myocardial infarction. Nat Med 2006;12:459–65.
[7] Nagaya N, Kangawa K, Itoh T, Iwase T, Murakami S, Miyahara Y, et al. Transplantation of mesenchymal stem cells improves cardiac function in a rat model of dilated cardiomyopathy. Circulation 2005; 112:1128–35.
[8] Kodama M, Matsumoto Y, Fujiwara M, Masani F, Izumi T, Shibata A. A novel experimental model of giant cell myocarditis induced in rats by immunization with cardiac myosin fraction. Clin Immunol Immunopathol 1990;57:250–62.
[9] Tanaka K, Honda M, Takabatake T. Redox regulation of MAPK pathways and cardiac hypertrophy in adult rat cardiac myocyte. J Am Coll Cardiol 2001;37:676–85.
[10] Kodama M, Matsumoto Y, Fujiwara M, Zhang SS, Hanawa H, Itoh E, et al. Characteristics of giant cells and factors related to the formation of giant cells in myocarditis. Circ Res 1991;69:1042–50.
[11] Fairweather D, Kaya Z, Shellam GR, Lawson CM, Rose NR. From infection to autoimmunity. J Autoimmun 2001;16:175–86.
[12] Cunningham MW. T cell mimicry in inflammatory heart disease. Mol Immunol 2004;40:1121–7.
[13] Kodama M, Hanawa H, Saeki M, Hosono H, Inomata T, Suzuki K, et al. Rat dilated cardiomyopathy after autoimmune giant cell myocarditis. Circ Res 1994;75:278–84.
[14] Wang JF, Yang Y, Wang G, Min J, Sullivan MF, Ping P, et al. Embryonic stem cells attenuate viral myocarditis in murine model. Cell Transplant 2002;11:753–8.
[15] Di Nicola M, Carlo-Stella C, Magni M, Milanesi M, Longoni PD, Matteucci P, et al. Human bone marrow stromal cells suppress T-lymphocyte proliferation induced by cellular or nonspecific mitogenic stimuli. Blood 2002;99: 3838–43.
[16] Tse WT, Pendleton JD, Beyer WM, Egalka MC, Guinan EC. Suppression of allogeneic T-cell proliferation by human marrow stromal cells: implications in transplantation. Transplantation 2003;75:389–97.
[17] Rollins BJ. Chemokines. Blood 1997;90:909–28.
[18] Fuse K, Kodama M, Hanawa H, Okura Y, Ito M, Shiono T, et al. Enhanced expression and production of monocyte chemoattractant protein-1 in myocarditis. Clin Exp Immunol 2001;124:346–52.
[19] Kolattukudy PE, Quach T, Bergese S, Breckenridge S, Hensley J, Altschuld R, et al. Myocarditis induced by targeted expression of the MCP-1 gene in murine cardiac muscle. Am J Pathol 1998;152:101–11.
[20] Ji JF, He BP, Dheen ST, Tay SS. Interactions of chemokines and chemokine receptors mediate the migration of mesenchymal stem cells to the impaired site in the brain after hypoglossal nerve injury. Stem Cells 2004;22:415–27.
[21] Wang L, Li Y, Chen J, Gautam SC, Zhang Z, Lu M, et al. Ischemic cerebral tissue and MCP-1 enhance rat bone marrow stromal cell migration in interface culture. Exp Hematol 2002;30:831–6.
[22] Damas JK, Eiken HG, Oie E, Bjerkeli V, Yndestad A, Ueland T, et al. Myocardial expression of CC- and CXC-chemokines and their receptors in human end-stage heart failure. Cardiovasc Res 2000;47:778–87.
[23] Damas JK, Aukrust P, Ueland T, Odegaard A, Eiken HG, Gullestad L, et al. Monocyte chemoattractant protein-1 enhances and interleukin-10 suppresses the production of inflammatory cytokines in adult rat cardiomyocytes. Basic Res Cardiol 2001;96:345–52.
[24] Ing DJ, Zang J, Dzau VJ, Webster KA, Bishopric NH. Modulation of cytokine-induced cardiac myocyte apoptosis by nitric oxide, Bak, and Bcl-x. Circ Res 1999;84:21–33.
[25] Hirota H, Chen J, Betz UA, Rajewsky K, Gu Y, Ross Jr J, et al. Loss of a gp130 cardiac muscle cell survival pathway is a critical event in the onset of heart failure during biomechanical stress. Cell 1999;97: 189–98.
[26] Gnecchi M, He H, Liang OD, Melo LG, Morello F, Mu H, et al. Paracrine action accounts for marked protection of ischemic heart by Akt-modified mesenchymal stem cells. Nat Med 2005;11:367–8.
[27] Lee JK, Zaidi SH, Liu P, Dawood F, Cheah AY, Wen WH, et al. A serine elastase inhibitor reduces inflammation and fibrosis and preserves cardiac function after experimentally-induced murine myocarditis. Nat Med 1998;4:1383–91.
[28] Ono K, Matsumori A, Shioi T, Furukawa Y, Sasayama S. Contribution of endothelin-1 to myocardial injury in a murine model of myocarditis: acute effects of bosentan, an endothelin receptor antagonist. Circulation 1999;100:1823–9.

JOURNAL OF MATERIALS SCIENCE: MATERIALS IN MEDICINE 17 (2006) 33–41

Observation and quantitative analysis of rat bone marrow stromal cells cultured *in vitro* on newly formed transparent β-tricalcium phosphate

NORIKO KOTOBUKI[1], DAISUKE KAWAGOE[2], DAISHIROU NOMURA[3], YOUICHI KATOU[1], KAORI MURAKI[1], HIROTAKA FUJIMORI[3], SEISHI GOTO[3], KOJI IOKU[2], HAJIME OHGUSHI[1,*]

[1]*Research Institute for Cell Engineering (RICE), National Institute of Advanced Industrial Science and Technology (AIST), 3-11-46 Nakouji, Amagasaki, Hyogo 661-0974, Japan*
E-mail: n.kotobuki@aist.go.jp

[2]*Graduate School of Environmental Studies, Tohoku University, Aoba 20, Aramaki, Aoba-ku, Sendai 980-8579, Japan*
E-mail: ioku@mail.kankyo.tohoku.ac.jp

[3]*Division of Applied Medical Engineering Science, Graduate School of Medicine, Yamaguchi University, 2-16-1 Tokiwadai, Ube, Yamaguchi 755-8611, Japan*

To observe living cell morphology on ceramics by light microscopy, we fabricated a new material—transparent β- tricalcium phosphate (*t*-βTCP) ceramic—for the purpose of serving as a tissue culture substrate. Bone marrow stromal cells (BMSCs) were obtained from rat femora and cultured on both *t*-βTCP ceramic disks and culture grade polystyrene (PS) dishes in an osteogenic medium. After 1 day of culture, cell attachment and spreading on both the *t*-βTCP and PS substrata were equally and clearly detected by ordinary light microscopy. After 14 days of culture, extensive cell growth, alkaline phosphatase (ALP) staining, and bone mineral deposition could be detected on both substrata. In addition, quantitative biochemical analyses revealed high DNA content, ALP activity, and osteocalcin content of these cultures. This experiment is significant in that all of the results were similarly observed on both the *t*-βTCP and PS substrata, indicating the excellent properties of βTCP ceramics for BMSCs culture towards osteogenic differentiation.

Introduction

Viable cells can be cultured in suitable scaffolds, and composites of such cells have already been clinically applied to patients. As examples, some polymers such as collagen combined with a variety of cultured cells are currently being used for cartilage and skin regeneration [1, 2], and ceramics combined with mesenchymal cells are being used for bone regeneration [3]. In our clinical cases, culturing a patient's derived mesenchymal cells on any of hydroxyapatite (HA), β-tricalcium phosphate (βTCP), or alumina ceramics has been used in treating patients having skeletal problems. In particular, before cell transplantation to the patients, we forced the mesenchymal cells to become osteoblasts followed by the formation of bone matrix on a ceramic surface [4, 5]. We have therefore defined the tissue-engineered construct fabricated by culturing mesenchymal cells on ceramics as *regenerative cultured bone tissue* [6].

Many researchers, ourselves included, have previously reported that composites of fresh bone marrow (without culture) and porous HA or βTCP [7–9] can show extensive new bone formation after *in vivo* implantation. We considered that the bone formation could be initiated on a ceramic surface by attaching mesenchymal cells from bone marrow. However, due to *in vivo* conditions, observation of the cells/ceramic interaction is difficult. In this regard, *in vitro* culturing of bone marrow stromal cells (BMSCs) on ceramic disks might be another approach for observing cells/ceramic interaction. Usually, cultured cells can be observed with

*Author to whom all correspondence should be addressed.

0957–4530

an ordinary microscope when the culture is on culture dishes. However, due to the opacity of the ceramics, microscopic observation of the cells on ceramics is very difficult. Scanning electron microscopy (SEM) or other techniques can be used to observe the cells on the ceramics, but these techniques usually require cell fixation by glutaldehyde, paraformaldehyde, or similar fixative solution, and the cells are no longer viable. Moreover, consecutive observation of the same specimen during the culture period is impossible.

If the ceramic were transparent, we could use an ordinary microscope for observation, which would enable us to detect cell attachment, spreading, proliferation, and differentiation cascade. Recently, it has been claimed that transparent ceramics are useful for the observation of cultured cells [10]. Transparent ceramics are mainly made by a spark plasma sintering process (SPS) [11]. SPS systems have many advantages such as rapid sintering, sintering with fewer additives, uniform sintering, low operating expense, and relatively easy operation compared to that of conventional systems using hot press (HP) sintering, hot isostatic pressing (HIP), or atmospheric furnaces.

β-TCP ceramics are known to be highly biodegradable. Porous types of β-TCP have attracted much attention within the field of bone reconstruction [12–15]. The rates of proliferation and differentiation of cultured cells on β-TCP ceramics have been demonstrated by biochemical analyses or gene expression analysis [16, 17] and SEM observation. However the ceramics used were opaque and direct observation was difficult to accomplish. Therefore, whether the surface of the ceramic could support cell attachment, proliferation, and differentiation was not clear. In this study, we made transparent βTCP (t-βTCP) ceramic disks (20 mm in diameter) using the SPS sintering method. We used rat BMSCs as the cell source and observed cell attachment, proliferation, and osteogenic differentiation on the t-βTCP ceramic disks as well as on culture grade polystyrene (PS) dishes as a positive control. PS dishes have been commonly used as cell culture substrates for a long time and their suitability is well known. This report describes not only the morphological but also the biochemical qualitative analyses of the BMSCs culture and includes a comparative study of the culture on t-βTCP and PS.

Materials and methods

Preparation of transparent βTCP (t-βTCP)

A fine powder made of βTCP (Taiheikagaku, Co. Ltd., Japan) was used as the basic material. One gram of this powder was poured into a graphite mold (inner diameter: 15 mm), and then sintered by the spark plasma sintering process (SPS: Dr Sinter-511S, Sumitomo Coal Mining, Tokyo, Japan). The samples were pressed uniaxially under 10 MPa, then heated at 1000 °C for 10 min at a heating rate of 25 °C/min. Each ceramic disk consisted of polycrystalline, transparent materials with a diameter of 20 mm and a thickness of 2 mm. The surface shapes and crystallographic analyses were determined using a scanning electron microscope (SEM, SM-300, Topcon Corporation, Tokyo, Japan) and an X-ray diffractometer (XRD, Geiger flex 2027, Rigaku, Japan), respectively.

Surface characterization

The surface roughness of the t-βTCP ceramic disks and PS dishes was measured by using a profilometer (Surfcorder SE-30D, Kosaka Lab., Ltd.) with a 5-μm tipped diamond stylus. Then, both the average roughness (Ra) and maximum roughness (Rz) were quantified. The sessile contact angles (SCA) of t-βTCP ceramic disks and PS dishes were determined using a Milli-Q water system and a goniometer (Face Contact-Angle Meter, Kyowa Kaimenkagaku Co., Ltd. Tokyo, Japan). A probability (p) of less than 0.05 was considered significant.

Cell culture

The preparation and osteogenic differentiation of bone marrow stromal cells (BMSCs) from 7-week-old male Fischer 344 (F344) rats were performed as described by Maniatopoulos *et al.* [18] with some modifications by us [19]. In brief, rat bone marrow plugs were flushed out and suspended in a culture medium, minimum essential medium (MEM, Nacalai Tesque, Inc., Kyoto, Japan) containing 15% fetal bovine serum (FBS, JRH Biosciences, Inc., KS, USA) and 1% antibiotics. These bone marrow cells were cultured in a humidified atmosphere of 95% air with 5% CO_2 at 37 °C.

The mesenchymal cells, which have osteogenic potentials, were contained in BMSCs. The adherent BMSCs were initially cultured up to 80% confluence in T-75 flasks, harvested, and resuspended to 5×10^5 cells/mL in culture medium using 0.05% trypsin/0.53 mM EDTA. One mL of cell suspension was applied to each sterilized t-βTCP ceramic disk (3.1 cm^2), which were placed into a 12-well PS plate (3.8 cm^2). As a control, the same amount of cell suspension was also applied directly in a PS well having no disks. These cells were cultured with osteogenic medium containing 10 nM dexamethasone (Dex, Sigma-Aldrich Corporation, MO, USA), 10 mM β-glycerophosphate (β-GP, Merck, Darmstadt, Germany), and 0.28 mM ascorbic acid 2-phosphate magnesium salt n-hydrate (AAc, Sigma-Aldrich Corp.). The culture medium was changed two or three times per week. During the culture period, the cell morphologies at different stages of cell attachment, proliferation, and differentiation were observed by light microscopy (Olympus CK41SF, Olympus Optical, Co., Ltd., Tokyo, Japan). Some cultures did not have Dex added but the other conditions were the same as above.

Qualitative biochemical analysis

Alkaline phosphatase (ALP) activity staining

At day 14, the cultured cells on both the *t*-βTCP ceramic disks and the PS dishes were rinsed with phosphate buffer saline (PBS) and fixed with 4% paraformaldehyde for 10 min at 4 °C. The fixed cells were soaked in 0.1% naphthol AS-MX phosphate and 0.1% fast red violet LB salt in 56 mM 2-amino-2-methyl-1, 3-propanediol (pH 9.9) for 10 min at room temperature and then washed with PBS.

Alizarin Red S staining

At day 14, the cultured cells on both the *t*-βTCP ceramic disks and the PS dishes were washed with PBS and fixed with 4% paraformaldehyde for 10 min at 4 °C. The fixed cells were soaked in 0.5% Alizarin red S /PBS for 10 min at room temperature and then washed with PBS. Non-specific reactions were removed by a wash step using 70% ethanol (EtOH). The stain was used to detect calcium in the extracellular matrix. To check a background level of Alizarin Red S, *t*-βTCP ceramic disks without cells were soaked into Alizarin red S in the same condition to cells (Fig. 6(e)).

Calcein uptake

The calcium in the extracellular matrix was also determined by using calcein, which is a calcium-chelating fluorescence chemical [20]. One μg/mL

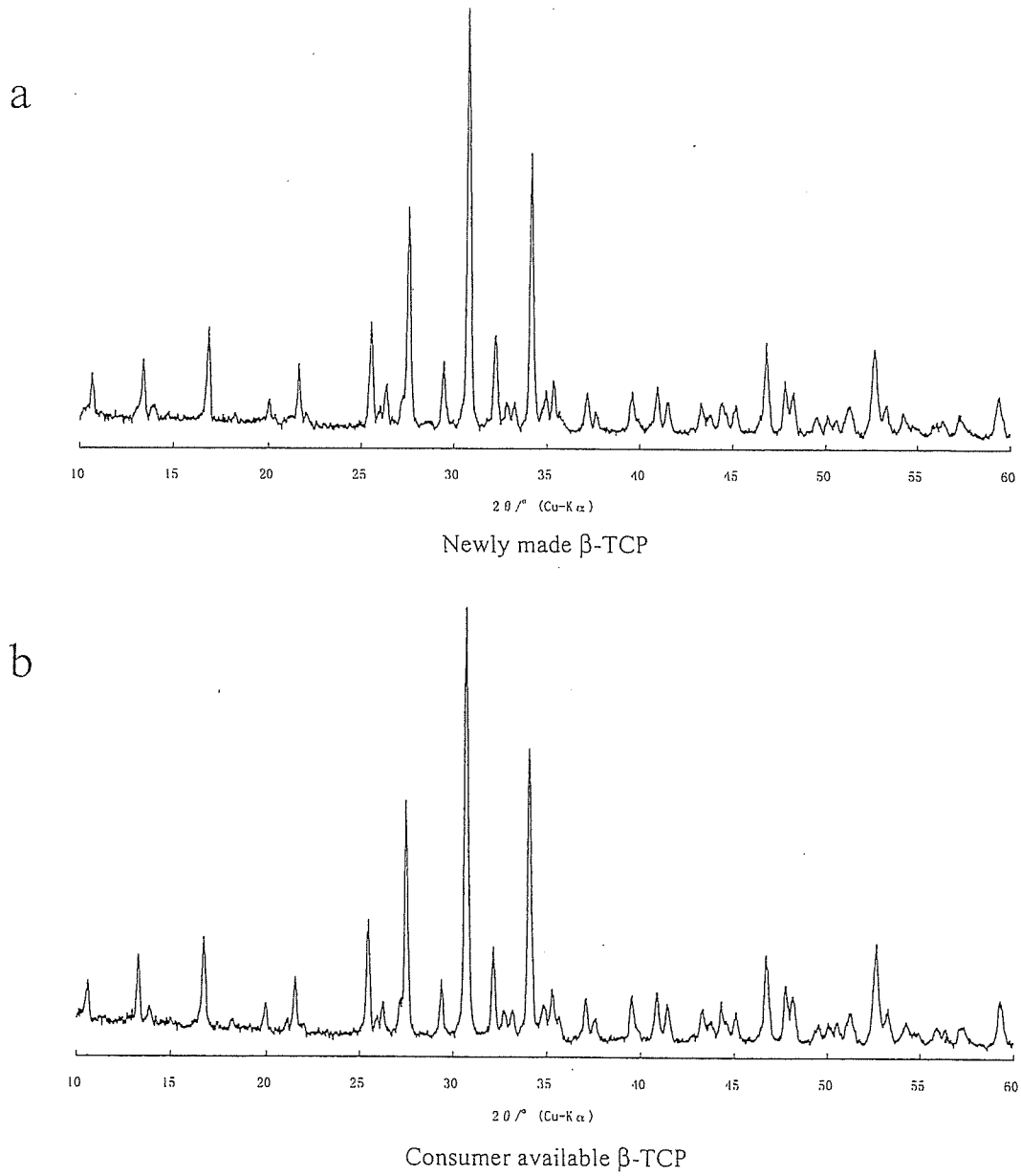

Figure 1 Powder X-ray diffraction (XRD) pattern of transparent βTCP ceramics made by spark plasma sintering (a) and standard βTCP (b). Details are given in the Materials and methods section.

calcein (Dojindo Laboratories, Kumamoto, Japan) was added to the medium during culture. The fluorescence of the incorporated calcein was observed by using a fluorescent microscope (IX70, Olympus). The medium containing calcein was removed and washed with PBS immediately before these analyses. To check a background level of calcein, t-βTCP ceramic disks without cells were soaked into medium containing calcein in the same condition to cells (Fig. 4(e)).

Quantitative biochemical analysis

Measurement of DNA contents

The DNA contents were measured by using Hoechst 33258 and expressed as $\mu g/cm^2$. The cells were scraped off the t-βTCP or PS surface into 0.5 mL of buffer (10 mM Tris-HCl, 1 mM EDTA and 100 mM NaCl (pH 7.4)) and sonicated. 20 μL of suspended cell solution was added to 0.2 mL of buffer containing 5 μg/mL Hoechst 33258 and the fluorescence was measured on a

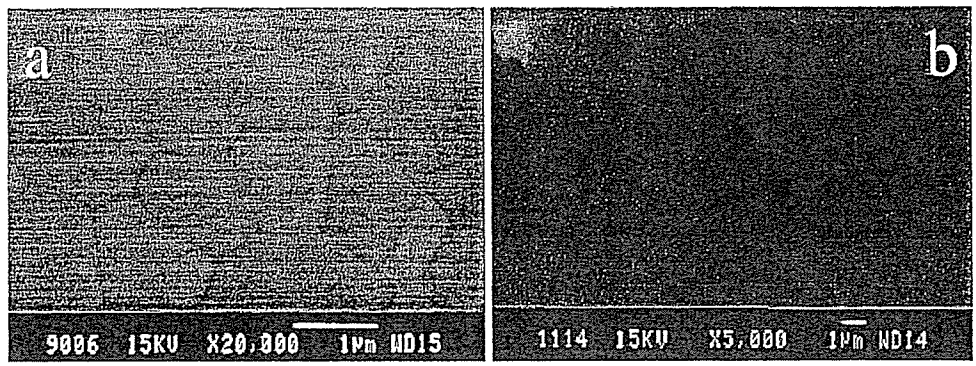

Figure 2 SEM images of transparent βTCP (a) and culture grade polystyrene (PS) (b) Bar: 1 μm. The surface of a culture grade PS dish is very smooth and, therefore, most of the SEM photos were out of focus. To bring the object into focus, we photographed a dish contaminated with a very small dust particle (shown at the upper left) as a pointer.

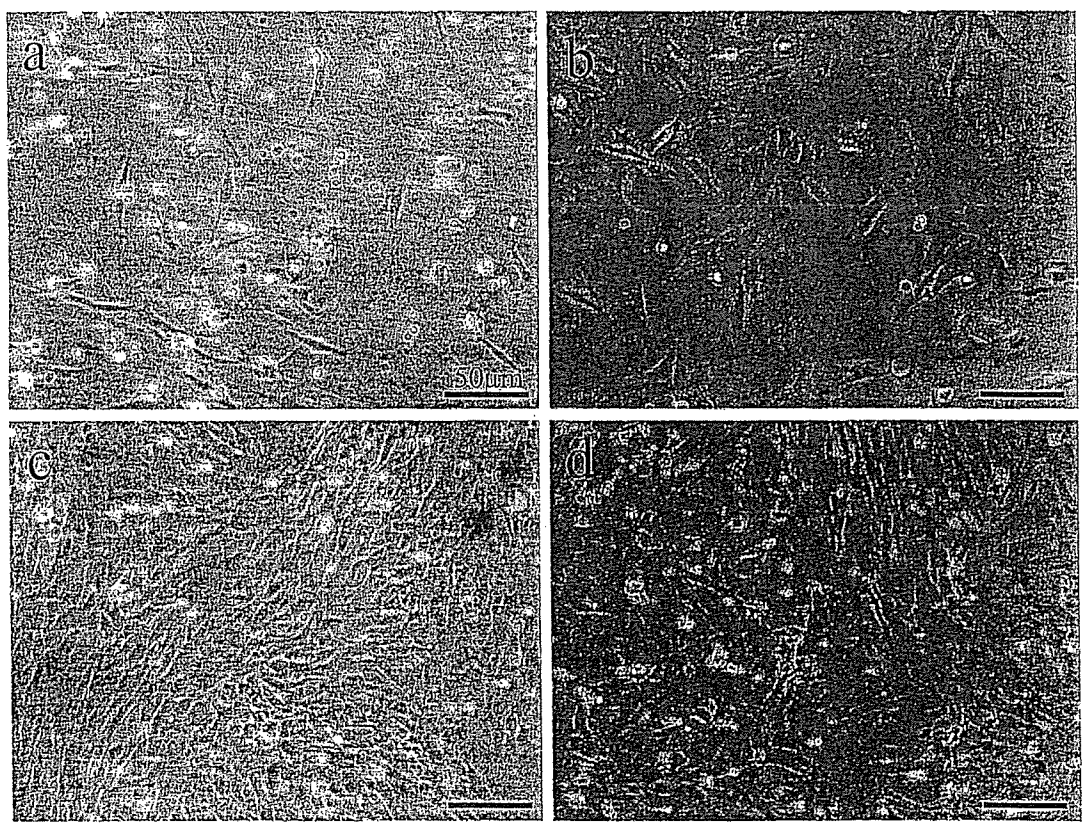

Figure 3 Cell morphology of rat BMSCs seeded on transparent βTCP ceramic disks and culture grade polystyrene (PS) dishes. The cells seeded on βTCP ceramic disks are shown in the left column (a, c). The cells seeded on PS dishes are shown in the right column (b, d). Bar: 50 μm. Cell morphology at day 1 (a, b) and day 4 (c, d) after BMSCs seeding on PS dishes and t-βTCP ceramic disks observed by light microscopy. One day after cell seeding, the cells began to spread on the surface. Cells on both substrata proliferated well and most cells had a fibroblastic shape after 4 days.

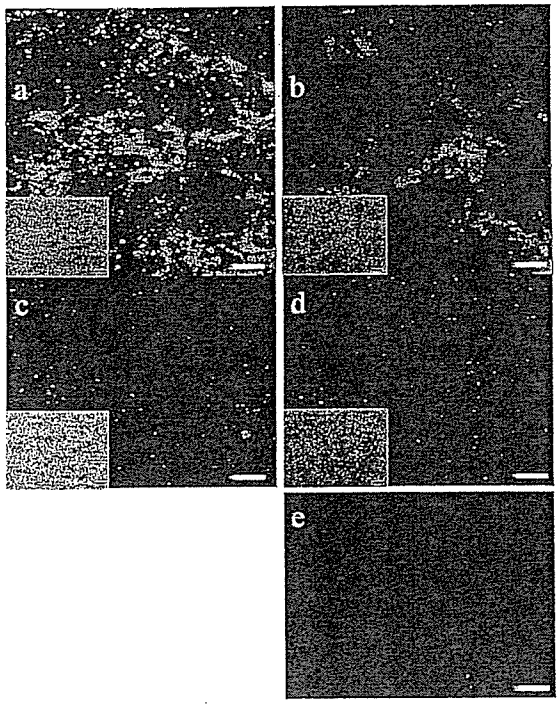

Figure 4 Calcein uptake by rat BMSCs seeded on transparent βTCP ceramic disks and culture grade PS dishes at day 14. Bar: 200 μm. When BMSCs were cultured in the presence of Dex, the culture on both culture grade PS dishes (a) and transparent βTCP (t-βTCP) ceramic disks (b) showed extracellular mineralization indicated by a green fluorescence. In contrast, in the absence of Dex, cells did not differentiate into osteoblasts and the green fluorescence was not detected (c, d). Each inset at lower left shows the phase contrast microscopic view of the corresponding field. Background level of calcein when t-βTCP without cells were soaked into calcein contained medium were shown in e.

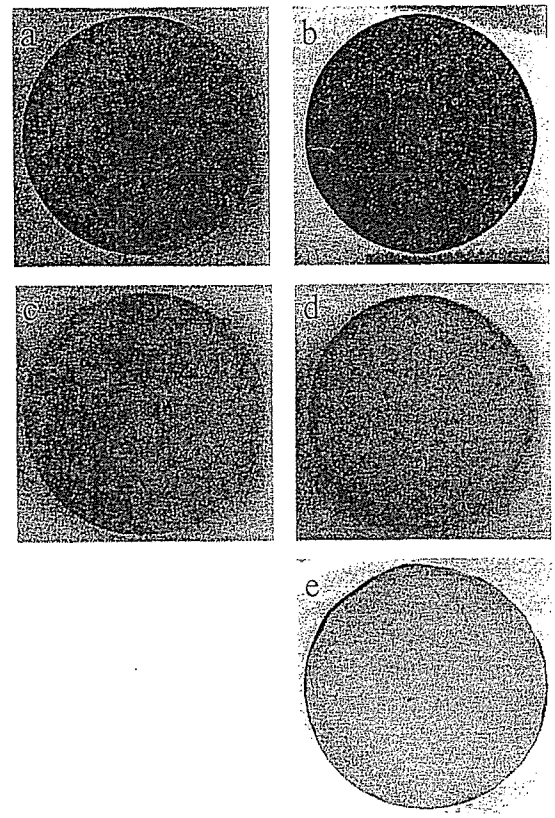

Figure 6 Macroscopic observation of ALP (a, c) and Alizarin Red S staining (b, d). When BMSCs were cultured in the presence of Dex (a, b), the cells on transparent βTCP differentiated into osteoblasts and showed extensive ALP (a) and Alizarin Red S (b) staining over the entire ceramics area compared with the control culture without Dex (c, d). Background level of Alizarin Red S when t-βTCP without cells were soaked into Alizarin Red S were shown in e.

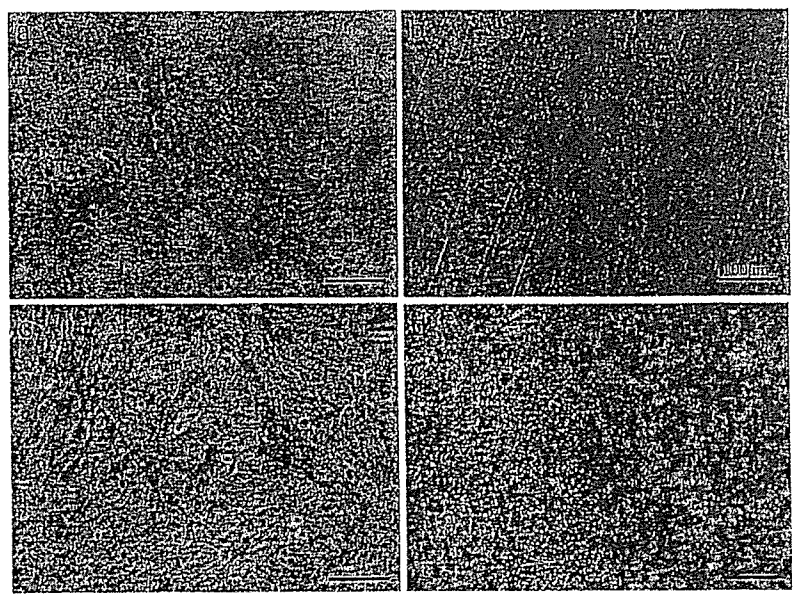

Figure 5 Microscopic observation of ALP and Alizarin Red S staining of the BMSCs culture. Bar: 100 μm. BMSCs were cultured in the presence of Dex for 14 days. Numerous regions of the cultured cells were positive for ALP on both t-βTCP ceramic disks (a) and PS dishes (c). Positive areas are represented in red. Strong Alizarin Red S stain could be detected in many cellular as well as extracellular regions on both the t-βTCP ceramic disks (b) and PS dishes (d).

micro plate reader (Wallac 1420 ARVOsx, PerkinElmer Life & Analytical Sciences, MA, USA). The standard DNA solutions were prepared using salmon sperm DNA (Invitrogen).

Alkaline phosphatase (ALP) activity assay

ALP activity of the cultured cells was examined quantitatively by the specific convention of *p*-nitro phenyl phosphate (pNPP) into *p*-nitro phenol (pNP). The cells were scraped off *t*-βTCP or PS surface into 0.5 mL of 10 mM Tris-HCl, 1 mM EDTA, and 100 mM NaCl (pH 7.4). The suspended cell solution was sonicated and centrifuged at 10,000 ×g for 1 min at 4 °C. An aliquot (20 μL) of the supernatant was assayed for ALP activity using PNPP solution (Zymed Laboratories Inc. CA, USA). The aliquot was incubated at 37 °C for 30 min. After enzymatic reaction was stopped with 0.2 M NaOH, the aliquot was measured for the absorbance of *p*-NP product formed at 405 nm on a micro plate reader (Wallac 1420 ARVOsx). Enzyme activity was expressed as μmol of pNP released/30 min/DNA content.

Measurement of Osteocalcin deposited in extracellular matrix by ELISA

The cells were scraped off and sonicated, then centrifuged at 10000 ×g for 10 min. After treatment of the precipitation in 20% formic acid for 2 days, the samples were centrifuged at 800 ×g for 10 min and the supernatants were subjected to gel filtration to eliminate inorganic ions. Gel-filtered samples were evaporated for concentration. The concentrated samples were added to an EIA plate and immobilized with anti-rat osteocalcin antibody to measure the concentration of osteocalcin with an intact rat osteocalcin EIA kit (Biomedical Technologies Inc. MA, USA). Osteocalcin deposition was expressed as ng/DNA content.

Results

Fig. 1(a) shows the X-ray diffraction (XRD) pattern of a spark plasma sintering (SPS) specimen of *t*-βTCP. The peaks in both figures clearly show that the specimen we made is similar to that of typical βTCP (Fig. 1(b)). We analyzed the surfaces of the *t*-βTCP ceramic disks by scanning electron microscopy (SEM) before the cell culture. Although the surfaces of the *t*-βTCP ceramic disks were slightly rough compared with the surfaces of the PS (Fig. 2(b)), the grain structure of the surface of the sintered *t*-βTCP ceramic disks was fine (less than 1 μm) (Fig. 2(a)).

It is well known that the surface roughness and wettability of culture substrata influence cell attachment and proliferation. The average roughness and maximum roughness of both the *t*-βTCP ceramic disks and the PS dishes were measured by using a profilometer (Table I). The roughness levels of the specimens were similar. We also checked the wettability of the *t*-βTCP ceramic disks and the PS dishes, which is represented by sessile contact angles (SCA) (Table I). The SCA of the *t*-βTCP ceramic disks and the PS dishes showed no significant difference. The results indicate that surface structure is not an important factor in comparing cellular responses on *t*-βTCP ceramic disks to that on PS dishes.

TABLE I Surface roughness and sessile contact angle of each culture substrate

	Surface roughness (μm)		
Material	Ra	Rz	SCA (°±SD)
Culture dish	0.005	0.040	71.0 ± 3.42
β-TCP	0.008	0.079	74.7 ± 3.92

We observed the cell attachment, spreading, and proliferation of rat BMSCs on both culture substrata during the early culture periods. Then, the capacity of BMSCs for osteogenic differentiation was investigated during the late culture periods. The *t*-βTCP ceramic disks are sufficiently transparent to perform microscopic observations and, thus, the cells cultured on the *t*-βTCP ceramic disks can easily be observed by light microscopy equal to those on PS dishes. At a very early stage of the culture, rat BMSCs attached, followed by spreading on not only the PS dishes but also on the *t*-βTCP ceramic disks. One day after the seeding, most of the cells were able to attach and exhibit the morphological characteristics of mesenchymal types (spindle cell morphology) (Fig. 3(a) and (b)). The cells proliferated well and almost all were spindle-shaped after 4 days on both substrata (Fig. 3(c) and (d)). It is thus suggested that rat BMSCs could easily attach, spread, and proliferate on *t*-βTCP ceramics as well as on PS.

In order to analyze the osteogenic differentiation of BMSCs, the BMSCs were further cultured on both *t*-βTCP ceramic disks and PS dishes in the presence of dexamethasone (Dex) for 14 days, and cell morphology was observed by light microscopy. Dex is used because it is well known as an osteogenic factor. To observe the extracellular mineralized matrix more clearly, we added calcein to the medium and measured its fluorescent intensity. When cultured in the osteogenic condition for 14 days, the same level of mineralized bone matrix on both the *t*-βTCP ceramic disks and the PS dishes was observed (Fig. 4(a) and (b)). In contrast, the BMSCs cultured in the absence of Dex showed no osteoblastic cell shape but did show a fibroblastic shape and no evidence of matrix formation (Fig. 4(c) and (d)). These findings indicate that BMSCs can easily differentiate into osteoblasts on the surface of *t*-βTCP ceramics, resulting in the formation of bone matrix under osteogenic

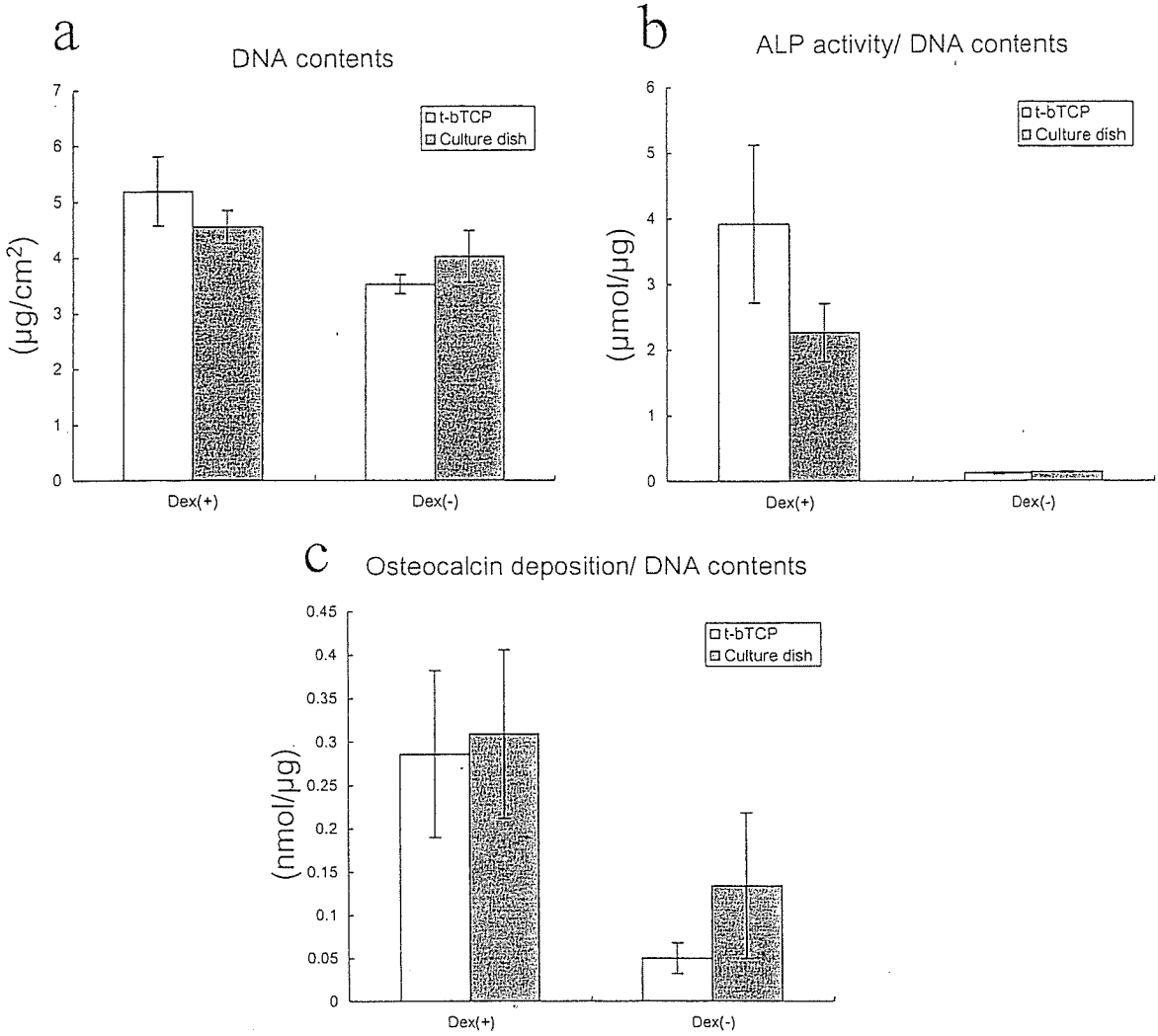

Figure 7 Quantitative and biochemical analyses of BMSCs cultured in the presence (+) or absence (−) of Dex. BMSCs were cultured on both transparent βTCP ceramic disks (t-βTCP) and culture grade polystyrene dishes (culture dish) for 14 days. The DNA contents were represented as micrograms per cm^2 (a). ALP activity (b) and osteocalcin deposition (c) were normalized for DNA content.

conditions. Importantly, the cascade of the differentiation of BMSCs can equally be observed on both t-βTCP ceramics and PS.

To confirm the osteogenic differentiation of BMSCs on the t-βTCP ceramic disks, we performed alkaline phosphatase (ALP) activity and Alizarin Red S staining after two weeks of cultivation. ALP, which is a cell surface protein, is known as an early marker for osteoblastic differentiation and Alizarin Red S can identify calcium in the matrix. Many clusters of cells were well stained with ALP on both the t-βTCP ceramic disks (Fig. 5(a)) and PS dishes (Fig. 5(c)) when cultured with Dex. As seen in the ALP stain, the cultures with Dex were strongly stained with Alizarin Red S (Fig. 5(b) and (d)). In contrast, the cultures without Dex were barely stained with either ALP or Alizarin Red S, as evidenced by macroscopic observation (Fig. 6). These biochemical data showed that the osteogenic differentiation of BMSCs cultured in the presence of Dex could occur on both t-βTCP ceramic and PS substrata.

After 14 days of culture, the DNA contents from each substrate were measured. The DNA contents were similar regardless of the culture substrata (Fig. 7(a)). As seen in ALP staining (Figs. 5 and 6) the cultures on both substrata with Dex showed high ALP activity compared with the culture without Dex (Fig. 7(b)). These data confirmed the morphological data (Figs. 3–6) that βTCP ceramics as well as PS supports the proliferation and osteogenic differentiation of BMSCs cultured in the presence of Dex. To confirm the osteogenic differentiation, we measured the bone-specific protein of osteocalcin. As seen in Fig. 7(C), high levels of osteocalcin were detected in the culture with Dex on both substrata. These quantitative biochemical data were evidence that the surfaces of both the t-βTCP ceramic disks and the PS dishes provide considerable

support for the osteoblastic differentiation cascade of BMSCs.

Discussion

In this study, cell behavior on transparent βTCP ceramic disks was compared with that on culture grade PS dishes. PS dishes are considered the gold standard substratum for cell cultivation and were therefore used in the present experiment as a positive control. It has also been reported that the surface characteristics of the culture substrata affect cell behavior during the culture period [21, 22]. As can be seen in Table I, the surface roughness and wettability of t-βTCP were similar to those of PS. It is considered that the optimum wettability for cell attachment is about 70 ° (defined by sessile contact angle; SCA), and the SCA of t-βTCP as well as PS is nearly 70 °. Additionally, the surface of t-βTCP is very smooth as is that of PS as observed by SEM (Fig. 2). These data mean that the wettability of t-βTCP is suitable for cell attachment and that surface roughness is not a decisive factor for comparing cell behavior on both substrata.

Currently, *in vitro* osteogenic differentiation on the various ceramics can be monitored by ALP staining or calcium staining after fixation as shown in Fig. 6. However, microscopic observation of this staining is difficult due to the opacity of ordinary ceramics. In addition, staining cannot be used for repeated monitoring of the same specimen during the culture period. In this regard, by using t-βTCP ceramic, we can detect the ALP and Alizarin Red S stain at the cellular level (Fig. 5). By adding calcein to the culture medium, we can clearly monitor the differentiation indicated by fluorescence emission (Fig. 4). Fluorescence can be detected repeatedly for the same specimen during the entire culture period. As seen in the results, we confirmed the capability of t-βTCP to enable BMSCs attachment, proliferation (Fig. 3), and osteogenic differentiation as confirmed by ALP stain, Alizarin Red S stain (Fig. 5), and calcein uptake (Fig. 4). We also confirmed that the capability of t-βTCP as a cell culture substrate was similar to that of PS. The qualitative analyses were confirmed by quantitative analyses of DNA, ALP activity, and osteocalcin measurements (Fig. 7). The data verify that the surface of t-βTCP ceramic is equivalent to that of culture-grade PS and has the capability of supporting cellular adhesion and proliferation, which results in the osteogenic differentiation of BMSCs. It is important to demonstrate a functional equivalence of both substrata because PS is suitable to *in vitro* culture but the appropriate materials for tissue engineering is βTCP. It is possible to make various type of βTCP combined with extracellular matrix or growth factors. And we can control a composition of βTCP. Together, we concluded that an observable transparent βTCP is useful materials for *in vitro* research in the field of medicine especially tissue engineering.

Conclusion

We fabricated a new material, a transparent βTCP (t-βTCP) ceramic, and used it as a culture substrate. The ceramic material enables the observation of cultured cells by light microscopy. The shape of the cells on the ceramic disks was as clearly detected as that seen on culture grade polystyrene (PS) dishes. In this report, rat bone marrow stromal cells (BMSCs) were cultured. As a result, cell attachment, proliferation, and differentiation of BMSCs on t-βTCP disks were similar to those on (PS) dishes. The results were confirmed by quantitative biochemical assay. All results confirmed the excellent properties of βTCP for supporting the differentiation capability of BMSCs, which resulted in osteoblastic phenotype expression.

Acknowledgments

We thank our colleagues at the National Institute of Advanced Industrial Science and Technology (AIST), at the Graduate School of Environmental Studies, Tohoku University, and at the Graduate School of Medicine, Yamaguchi University. And we especially thank Dr. Oshimura at the Graduate School of Medical Sciences, Tottori University for valuable discussion. The Three-Dimensional Tissue Module Project of METI (a Millennium Project) and Grant-in-Aid for Scientific Research Japan supported this work.

References

1. S. WAKITANI, K. IMOTO, T. YAMAMOTO, M. SAITO, N. MURATA and M. YONEDA, *Osteoarthritis Cartilage* **10** (2002) 199.
2. M. OCHI, Y. UCHIO, K. KAWASAKI, S. WAKITANI and J. IWASA, *J. Bone Joint Surg. Br.* **84** (2002) 571.
3. R. QUARTO, M. MASTROGIACOMO, R. CANCEDDA, S. M. KUTEPOV, V. MUKHACHEV, A. LAVROUKOV, E. KON and M. MARCACCI, *N. Engl. J. Med.* **344** (2001) 385.
4. H. OHGUSHI and A. I. CAPLAN, *J. Biomed. Mater. Res.* **48** (1999) 913.
5. H. OHGUSHI, J. MIYAKE and T. TATEISHI, *Novartis Found Symp.* **249** (2003) 118.
6. N. KOTOBUKI, M. HIROSE, Y. TAKAKURA and H. OHGUSHI, *Artif. Organs* **28** (2004) 33.
7. H. OHGUSHI, M. OKUMURA, S. TAMAI, E. C. SHORS and A. I. CAPLAN, *J. Biomed. Mat. Res.* **24** (1990) 1563.
8. H. OHGUSHI, M. OKUMURA, T. YOSHIKAWA, K. INOUE, N. SENPUKE and S. TAMAI, *ibid.* **26** (1992) 885.
9. T. UEMURA, J. DONG, Y. WANG, H. KOJIMA, T. SAITO, D. IEJIMA, M. KIKUCHI, J. TANAKA and T. TATEISHI, *Biomaterials.* **24** (2003) 2277.
10. N. KOTOBUKI, K. IOKU, D. KAWAGOE, H. FUJIMORI, S. GOTO and H. OHGUSHI, *ibid.* (in press)
11. K. IOKU, D. KAWAGOE, H. TOYA, H. FUJIMORI, S. GOTO, K. ISHIDA, A. MIKUNI and H. MAE, *Trans. Mater. Res. Soc. Japan* **27** (2002) 447.